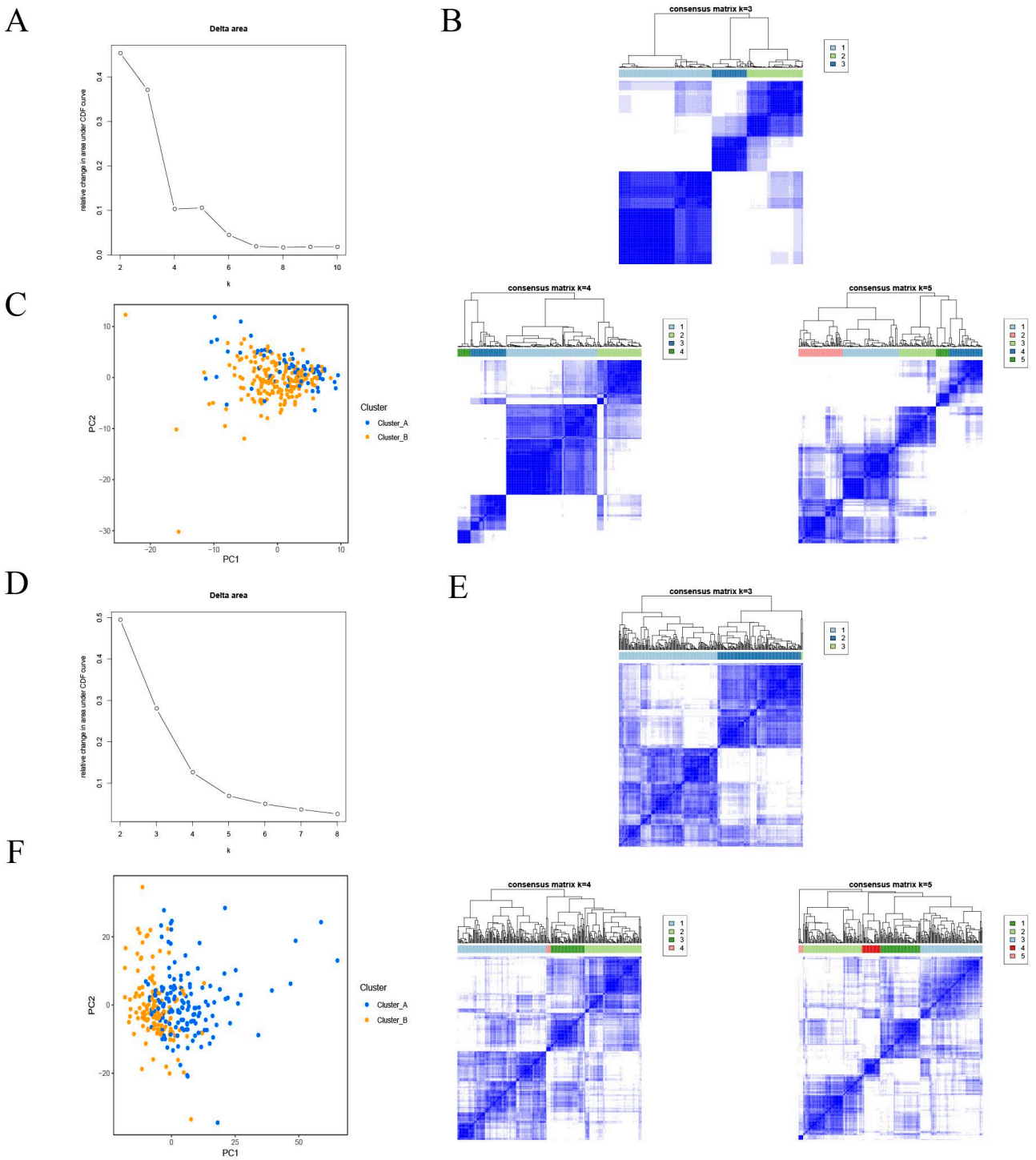

Figure S1 Consensus clustering of CC in TCGA and GEO cohorts. (A) Changes of slope and length of CDF curve when index k ranges from 2 to 10 in TCGA set. (B) Consensus clustering (k=3–5) using 258 metabolism-related genes in 253 CC from TCGA as a training set. (C) PCA showing the distribution of two CC clusters in training set. (D) Changes of slope and length of CDF curve when index k ranges from 2 to 10 in GEO set. (E) Consensus clustering (k=3–5) using 218 metabolism-related genes in 272 CC from GEO as a test set. (F) PCA showing the distribution of two CC clusters in training set.

https://dx.doi.org/10.21037/tcr-2024-2208

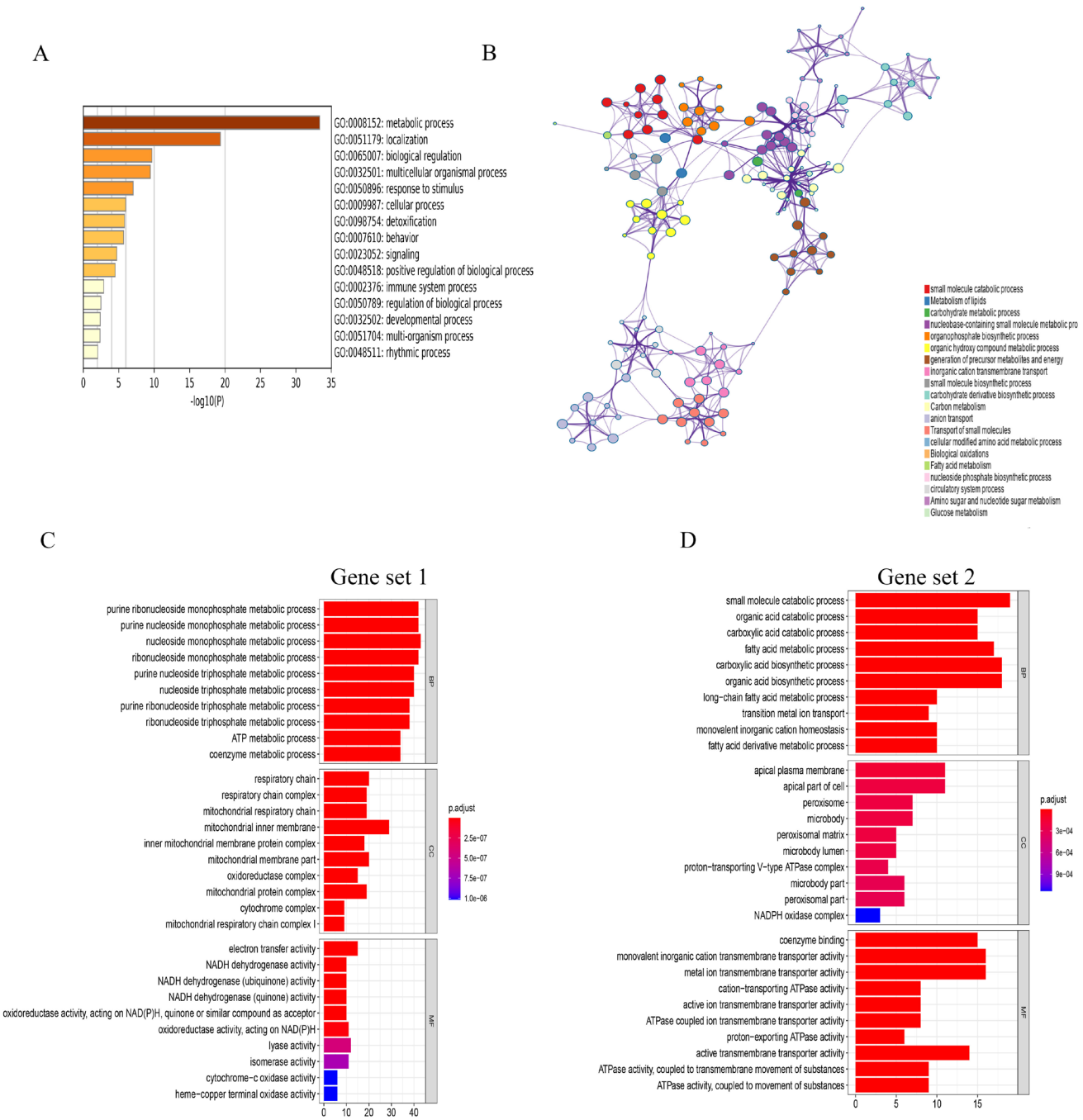

Figure S2 The functional analysis between two clusters. (A) GO analysis of the 258 significant metabolism-related genes. (B) The top pathway enriches of 218 significant metabolism-related genes. (C) GO analysis of significant metabolism-related genes in cluster_A. (D) GO analysis of significant metabolism-related genes in cluster_B.

https://dx.doi.org/10.21037/tcr-2024-2208

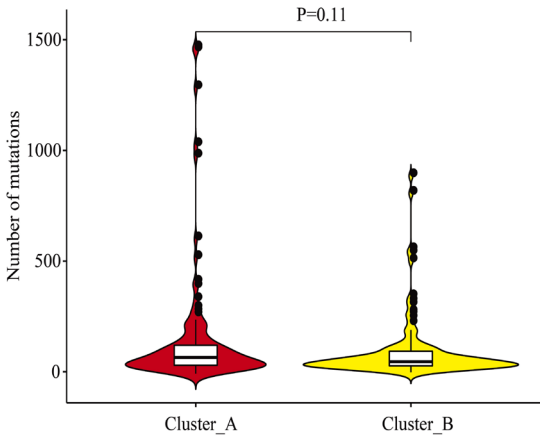

Figure S3 The comparison of mutation number between two clusters.

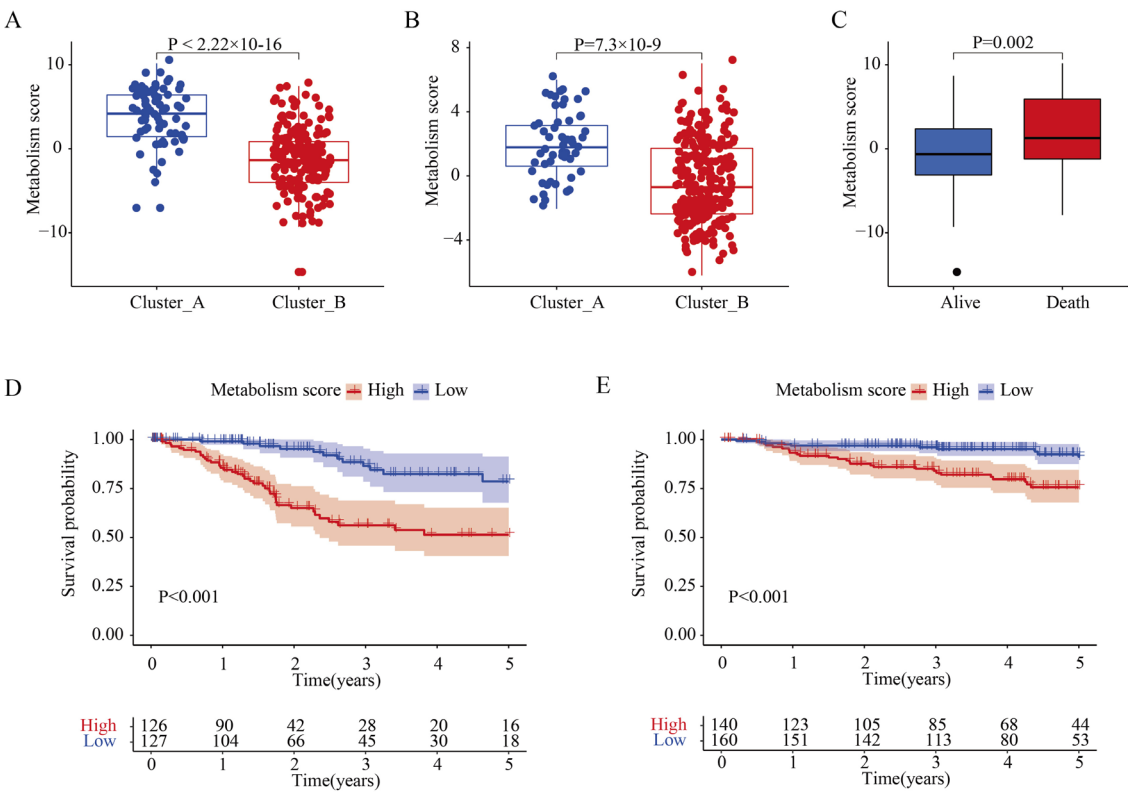

Figure S4 The difference of metabolism score and prognosis between two clusters (A) The difference of metabolism score between cluster_A and cluster_B in training set. (B) The difference of metabolism score between cluster_A and cluster_B group in test set. (C) The association of metabolism score with survival status. (D) Kaplan-Meier curves of patients' OS in the low- and high-metabolism score in training set. (E) Kaplan-Meier curves of patients' OS in the low- and high-metabolism score in test set.

https://dx.doi.org/10.21037/tcr-2024-2208

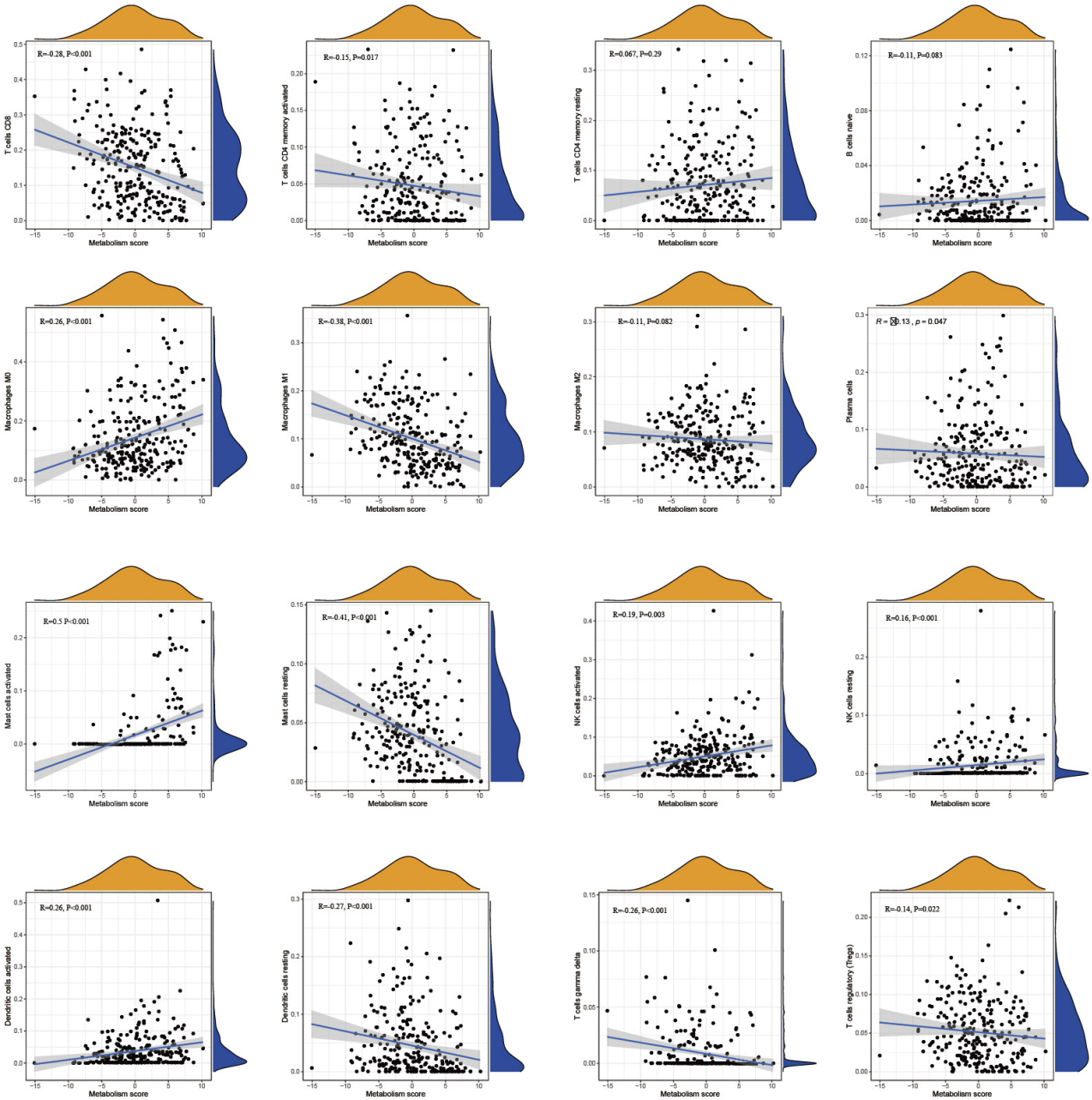

Figure S5 The association of metabolism score and immune cells.

https://dx.doi.org/10.21037/tcr-2024-2208

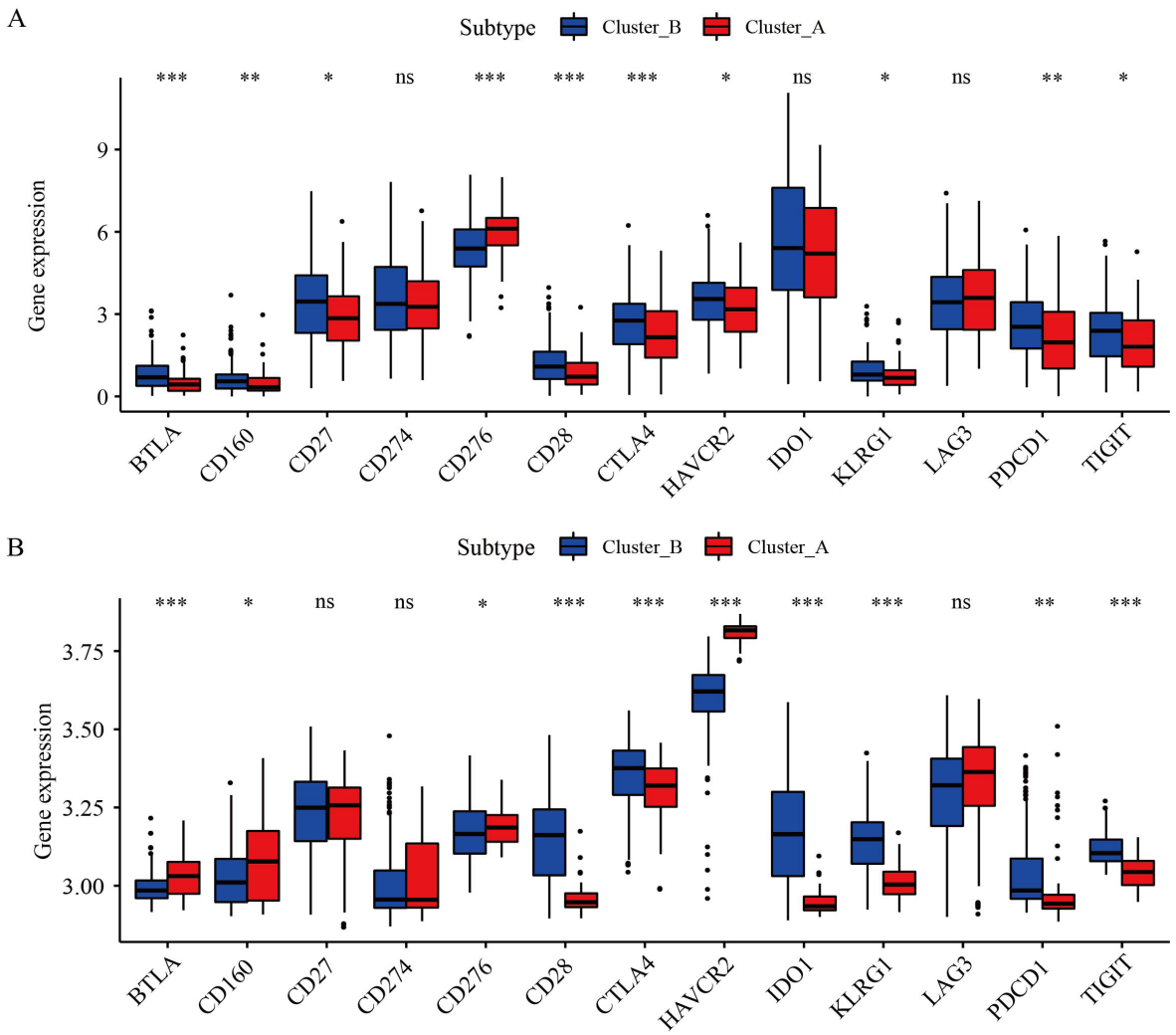

Figure S6 The difference of immune checkpoint genes expression between two clusters. The comparison of immune checkpoint genes between two clusters in training set (A) and test set (B). *, P<0.05; **, P<0.01; ***, P<0.001.

https://dx.doi.org/10.21037/tcr-2024-2208

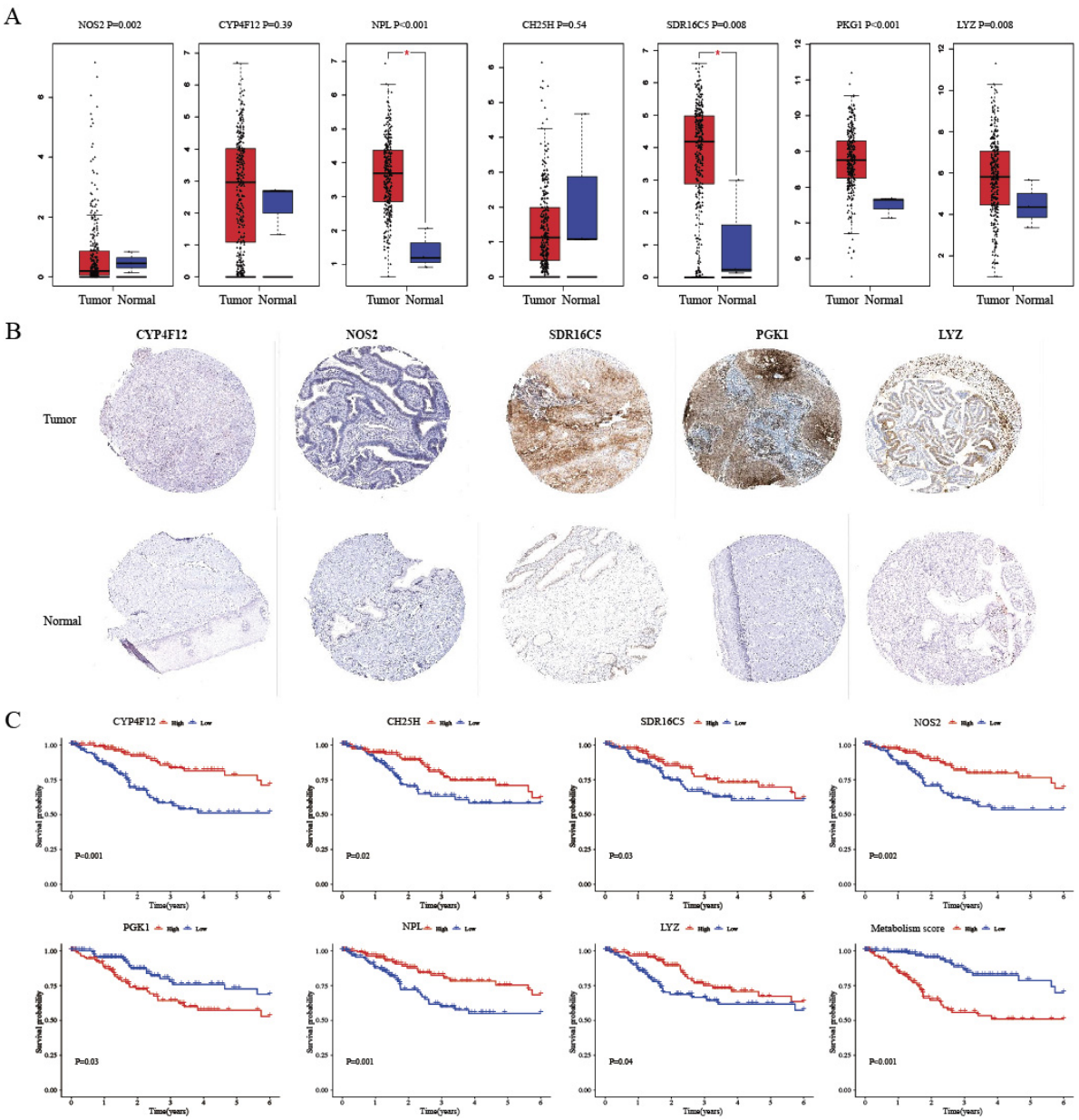

Figure S7 The expression difference of metabolism-related genes using RNA-seq data and protein data. (A) The expression difference of 7 significant metabolism-related genes between tumor tissue and normal cervical tissue by using RNA-Seq data (GEPIA website). (B) Translational level validation of five genes signature using the Human Protein Atlas (HPA). The link to the individual normal and tumor tissue of each protein were provided for CYP4F12 (https://www.proteinatlas.org/ENSG00000186204-CYP4F12/tissue/cervix#img; https://www.proteinatlas.org/ENSG00000186204-CYP4F12/cancer/cervical+cancer#img), NOS2 (https://www.proteinatlas.org/ENSG00000007171-NOS2/tissue/cervix#img; https://www.proteinatlas.org/ENSG00000007171-NOS2/cancer/cervical+cancer#img), SDR16C5 (https://www.proteinatlas.org/ENSG00000170786-SDR16C5/tissue/cervix#img; https://www.proteinatlas.org/ENSG00000170786-SDR16C5/cancer/cervical+cancer#img), PKG1 (https://www.proteinatlas.org/ENSG00000185532-PKG1/tissue/cervix#img; https://www.proteinatlas.org/ENSG00000185532-PRKG1/cancer/cervical+cancer#img) and LYZ (https://www.proteinatlas.org/ENSG00000090382-LYZ/tissue/cervix#img; https://www.proteinatlas.org/ENSG00000090382-LYZ/cancer/cervical+cancer#img). (C) Kaplan-Meier curves showing the impact of expression level of 7 significant metabolism genes and metabolism score with overall survival.

https://dx.doi.org/10.21037/tcr-2024-2208

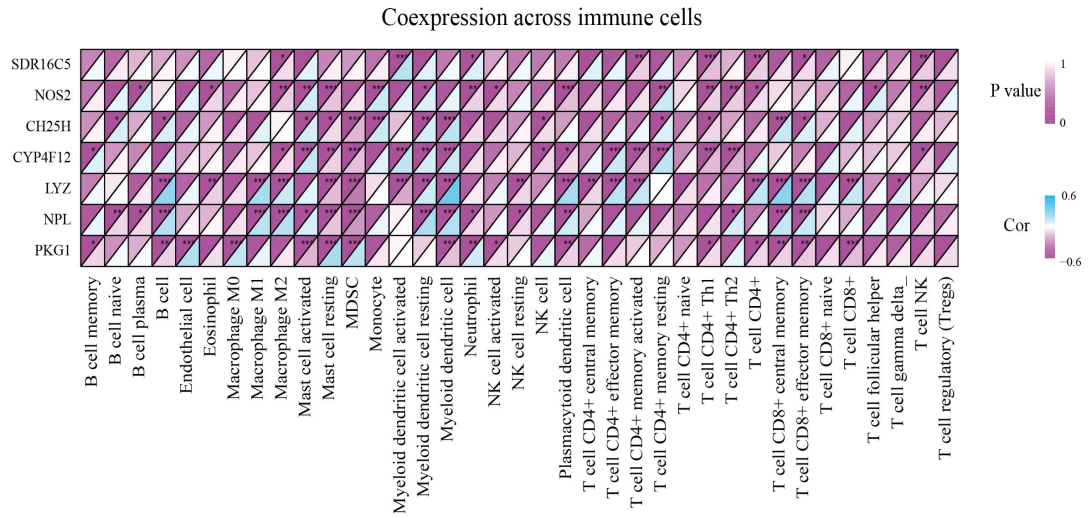

Figure S8 The correlation between the hub genes and various immune cells. *, P<0.05; **, P<0.01; ***, P<0.001.

https://dx.doi.org/10.21037/tcr-2024-2208

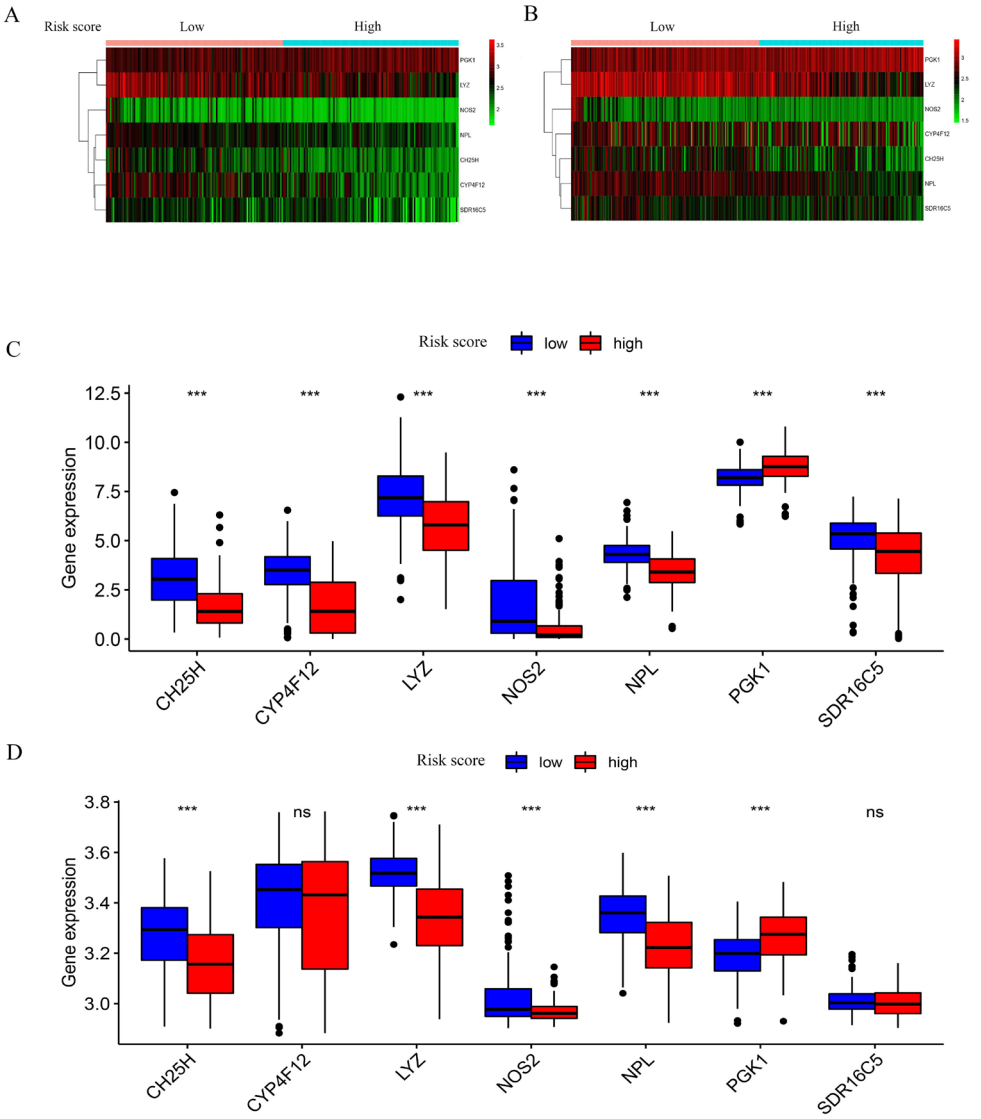

Figure S9 The expression difference of metabolism-related genes between high- and low-risk group. (A) Heatmap of expression profiles of 7 significant metabolism-related genes in training set. (B) Heatmap of expression profiles of 7 significant metabolism-related genes in test set. (C) Boxplot of the difference of 7 genes between high- and low-risk group in training set. ***, P<0.001. (D) Boxplot of the difference of 7 genes between high- and low-risk group in test set. ***, P<0.001.

https://dx.doi.org/10.21037/tcr-2024-2208

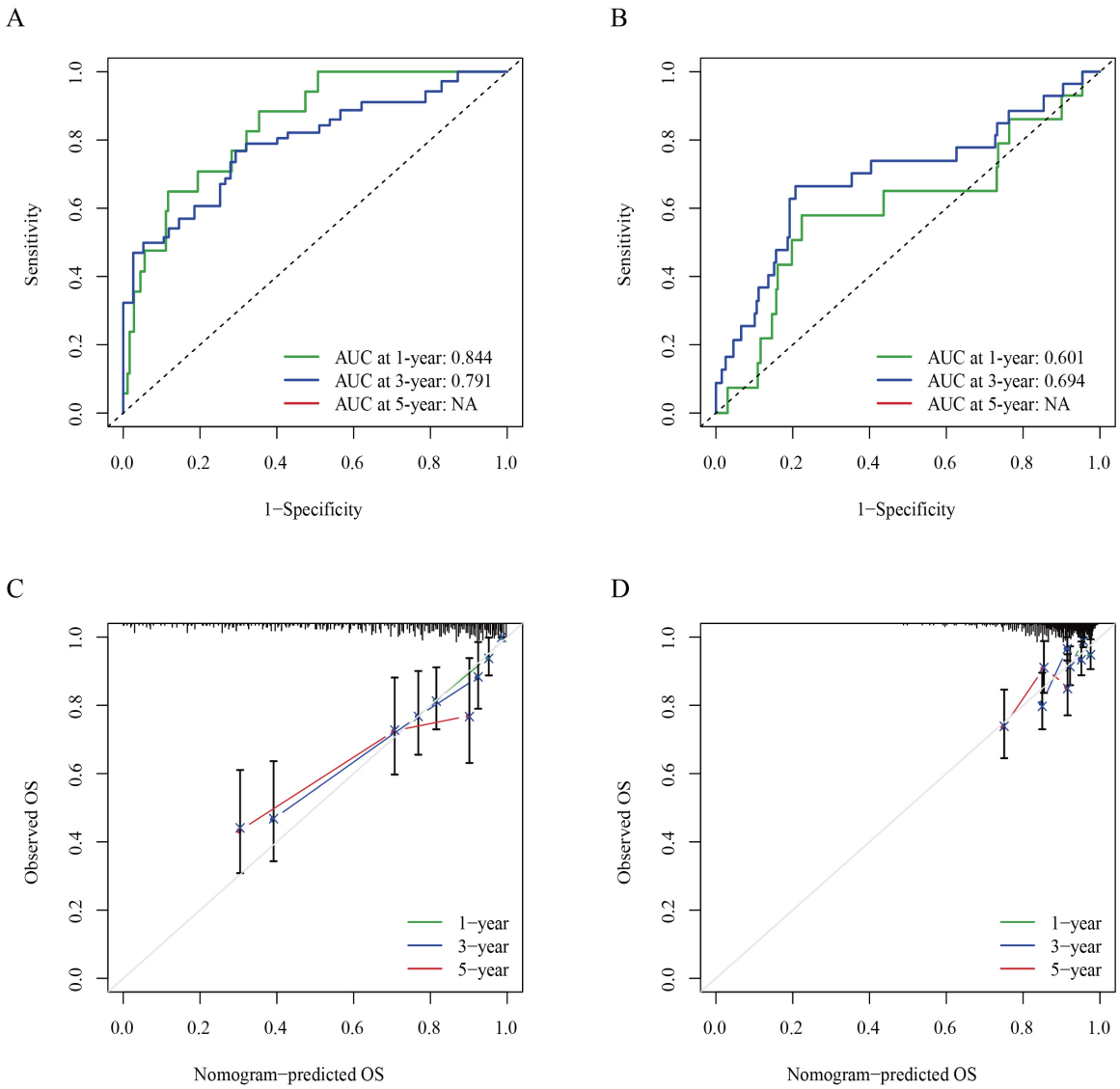

Figure S10 The validation of nomogram model. (A) ROC curve of the prognostic index mode in training set. (B) ROC curve of the prognostic index mode in test set. (C) The calibration plot for internal validation of the prognostic index mode in training set. (D) The calibration plot for internal validation of the prognostic index mode in test set.

https://dx.doi.org/10.21037/tcr-2024-2208

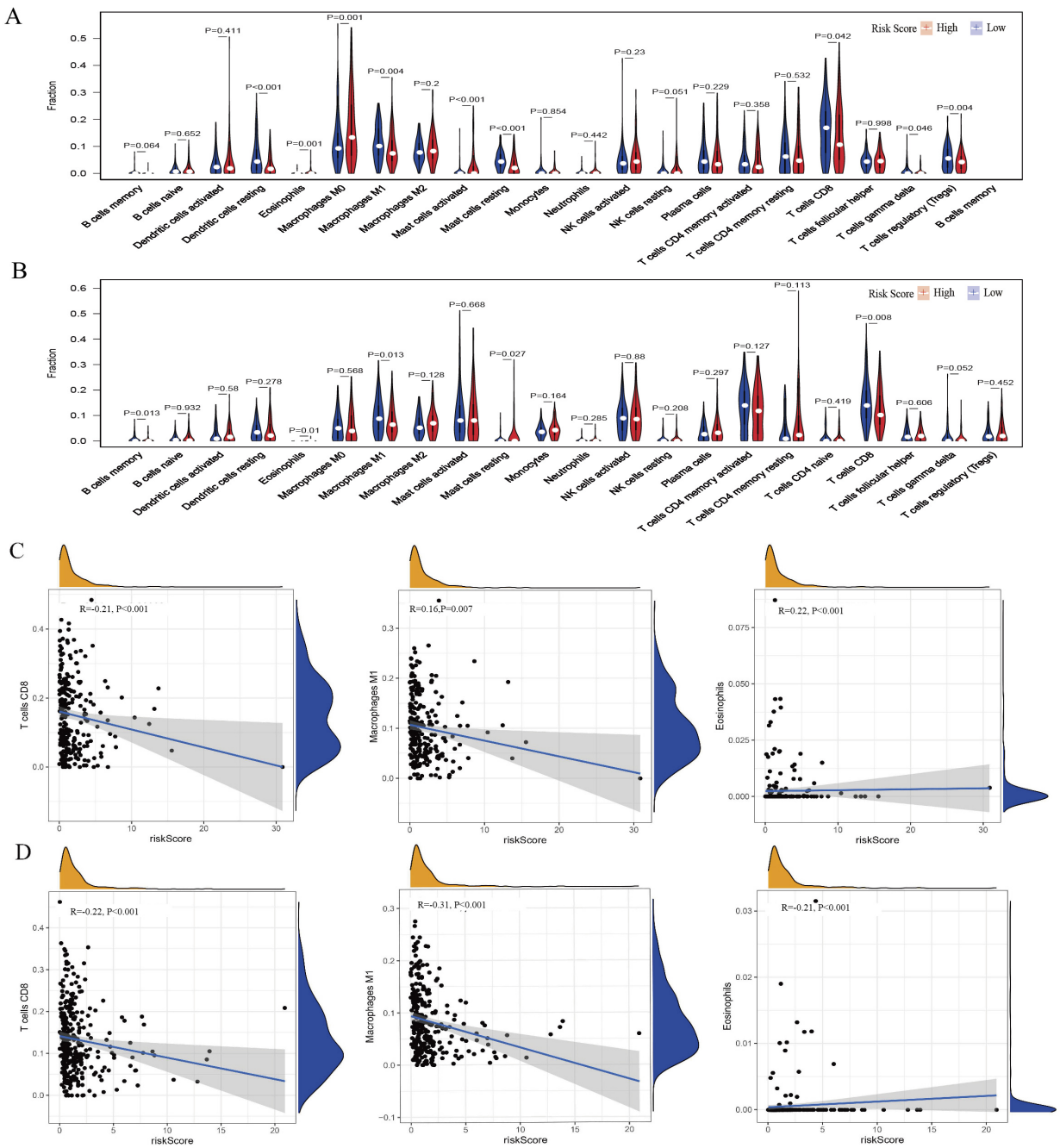

Figure S11 The association of immune cells with metabolism score. (A) Boxplot of the abundance of immune cell populations distinguished by high- and low-risk group in training set. (B) Boxplot of the abundance of stromal and immune cell population distinguished by high- and low-risk group in test set. The correlation of risk score with immune cells in training set (C) and in test set (D).

https://dx.doi.org/10.21037/tcr-2024-2208

Table S1 Characteristic of seven metabolism-associated genes and their function with metabolism and immune system

Gene	Full name	Description	Metabolic regulation	Immune regulation
CYP4F12	Cytochrome P450 family 4 subfamily F member 12	It belongs to the cytochrome P450 4F subfamily and constitute a multi-gene family of constitutive and inducible heme-containing key oxidative enzymes	It is association with the biosynthesis and degradation of steroids, vitamins, fatty acids, arachidonic acid, prostaglandins, amines, pheromones, and plant metabolites	It has the emergence of antitumor response by M1-polarized macrophages or lead to tumor-mediated immunosuppression
CH25H	Cholesterol 25-hydroxylase	It belongs to the redox enzyme family and consists of 298 and 272 amino acids in human and mouse cells, respectively and is mainly localized in the endoplasmic reticulum (ER) and Golgi apparatus and catalyzes the oxidation of cholesterol to 25HC	It has a well-defined role in the regulation of sterol biosynthesis, reducing cholesterol accumulation, thus executing its antiviral cellular functions and may do so also by repressing SREBP2 activation that regulates hepatic lipid homeostasis	It is potently expressed in macrophages and dendritic cells in response to activation of toll-like receptors (TLRs), through the production of type I and II IFNs
NOS2	Nitric oxide synthase 2	INOS gene is localized on chromosome 17q11.2-q12and generates NO by utilizing L-arginine as substrate, reduced nicotinamide-adenine-dinucleotide phosphate (NADPH) as co-substrate	It is capable of inhibiting numerous key enzymes containing iron in their catalytic centers such as complexes I and II, ribonucleotide reductase, because it tends to interact with protein bound iron	iNOS can be expressed in macrophages, it generates great amounts of NO resulting in critical cytotoxic responses. Greater amounts of NO generated in macrophage cells may interact with DNA of the cells and result in DNA strand breaks
SDR16C5	Short chain dehydrogenase/ reductase family 16C member 5	RDHE2 (SDR16C5) is known to recognize all-trans-retinol as a substrate with NAD+ as the preferred cofactor	It promotes retinoic acid biosynthesis when expressed in mammalian cells	–
PGK1	Phosphoglycerate kinase 1	PGK1 is an essential enzyme to produce ATP in the glycolytic pathway and has many characteristics of oncogene, promoting the tumor cell proliferation, migration and invasion, and playing vital roles in the progression of various tumors	PGK1 was often accompanied with an increase of glycolysis-related enzymes and CXCR4 in the renal cancer tissues	High PGK1 levels exhibited prominent correlations to immune checkpoints and high response to immunotherapy across pan-cancer
LYZ	Lysozyme	It is a naturally occurring enzyme that operates against Gram-positive bacteria and leads to cell death	LYZ levels in obesity has recently been associated with hyperglycemia, insulin resistance, dyslipidemia and inflammatory parameters	LYZ is an antimicrobial protein found in granules of neutrophils and macrophages and in a wide diversity of biological fluid. It is an important immune effector that carries out immunomodulatory activities, which trigger a proper response of innate immune system
NPL	N-acetylneuraminate pyruvate lyase	It encodes for N-acetylneuraminate pyruvate lyase, an enzyme regulating the cellular concentrations of N-acetyl-neuraminic acid (sialic acid) and was thought to play an important role in controlling the intracellular concentration of sialic acid	NPL catalyzes the breaking of carbon-carbon bonds of N-acetylneuraminic acid into N-acetylmannosamine and pyruvate, thus regulating the cellular concentrations of sialic acid and preventing the recycling of sialic acid for further sialylation with glycoconjugates	–

https://dx.doi.org/10.21037/tcr-2024-2208